Journal of Engineering Science and Technology
Vol. 13, No. 6 (2018) 1489 - 1499

STATIC STRUCTURAL PERFORMANCE OF CONTINUOUS COMPOSITE SLAB STRENGTHENED BY CFRP LAMINATE IN THE HOGGING MOMENT REGION

KHALID W. DAHHAM, SHAHRIZAN BAHAROM*,
WAN HAMIDON W. BADARUZZAMAN,
NORHASNI MUHAMMAD, AHMED W. AL-ZAND

Smart and Sustainable Township Research Centre,
Faculty of Engineering and Built Environment, Universiti Kebangsaan Malaysia,
UKM 43600, Bangi, Selangor DE, Malaysia
*Corresponding Author: shahrizan@ukm.edu.my

Abstract

The performance of continuous composite deck slab (CCS) strengthened with unidirectional carbon fibre-reinforced polymer (CFRP) laminate in the hogging region was investigated in this study, where the CFRP worked as an external reinforcement in the concrete tension region. Four specimens of CCS that consisted of two equal spans were tested experimentally under static loads after strengthening with CFRP laminates of varying lengths. The test results confirmed that the hogging moment capacity of the CCS was improved significantly when the CFRP length was increased. However, CFRP debonding failure occurred in all strengthened specimens, and increasing the CFRP length did not totally prevent the debonding failure from occurring, although it did delay this failure somewhat. The CCS specimens absorbed more energy when strengthened with the CFRP laminates.

Keywords: CFRP, Continuous composite slab, Debonding, Energy absorption, Hogging moment.

1. Introduction

In the last few years, composite steel floor deck-slab systems have been commonly used in modern projects (multi-story buildings, factories, and bridges), since they can achieve sufficient strength capacity with high ductility behaviour. The profiled steel sheets (steel deck) in this composite slab system can be used as permanent shuttering during the casting stage of concrete, and thus use of the system can speed up construction works at a lower cost compared to a conventional concrete slab

Nomenclatures

E	Modulus Young
EA	Energy absorption
f_{cu}	Compressive strength of concrete
f_t	Tensile strength
M_d	Moment value at debonding
M_u	Ultimate moment
t	Thickness

Greek Symbols

ε	Material ultimate strain in tension

Abbreviations

CCS	Continuous Composite Deck Slab
CFRP	Carbon Fibre-Reinforced Polymer
LIR	Load Improvement Ratio

system. In general, the longitudinal shear-bond resistance between the profiled steel sheets and concrete has a major effect on the behaviour and strength capacity of the simply supported composite slab [1-4].

However, in the case of the continuous composite slab (CCS), there are two types of moments, usually called the sagging moment, located in the mid-span region of the slab, and the hogging moment, located at the intermediate supports. The bending moment in the sagging region can be controlled by a profile steel sheet which acts to resist tensile forces, while the negative bending moment in the hogging region (intermediate supports) can be controlled by providing additional reinforcement bars at the top of the slab [2, 5-6]. Furthermore, the negative moment capacity of the CCS at the intermediate supports is small, especially when a limited reinforcement ratio is provided at the top of the concrete part [7]. The absence of reinforcement bars in the hogging moment region usually leads to a sudden redistribution of the moment at the first crack in the concrete, and later, one or more large unserviceable cracks will develop [5]. EC4 [2] recommends that the continuous slab should be designed in the same way as the simply supported slabs, where it is necessary to provide anti-crack reinforcement bars in the top portion with not less than 0.2% of the concrete cross-sectional area above the sheet's ribs.

Recently, several research works have investigated the efficiency of using Carbon Fibre-Reinforced Polymer (CFRP) laminate composite material to strengthen and repair reinforced concrete and composite structural members. CFRP laminate has high strength and a high modulus of elasticity compared to its weight ratio, has sufficient corrosion resistance, and is easy to handle and apply. In general, numerous experimental studies have proved the validity of using CFRP laminates/plates to strengthen reinforced concrete slabs and beams, such as [8-10]. Ashour et al. [8] used an analytical method to estimate the flexural strength of continuous reinforced concrete beams externally bonded with CFRP laminates, which were placed at the upper and lower limits of the beam. Kim et al. [9] experimentally investigated the behaviour of the continuous reinforced concrete slab (a polymeric hybrid composite system made of high-performance concrete) when strengthened with unidirectional CFRP laminates.

The results of this study indicated that the load capacity of the hybrid retrofit system improved by about 130%, and it also converted the brittle shear failure mode of the slab to a desirable ductile flexural failure mode. Meanwhile, limited studies have investigated the strengthening behaviour of composite structures using CFRP laminates. In the case of a composite beam system, an experimental and non-linear finite element (FE) analysis to investigate the behaviour of steel-concrete composite beams stiffened in the hogging moment region with CFRP sheets was carried out by El-Shihy et al. [10]. A total of five specimens were tested under two-point loads. Three of the composite beams included concrete slab only (steel I-beams with concrete slab), while the other two beams had composite deck-slabs (steel I-beam with concrete deck-slab). The study confirmed that all the strengthened models exhibited a higher load capacity than the control models (unstrengthened beams), but with lower ductility behaviour. Also, increasing the length of CFRP laminates to cover the entire negative (hogging) or positive (sagging) moment zones did not prevent peeling failure.

The use of CFRP in CCS system could minimise or eliminate the use of reinforcement bar in hogging region, which could lead the reduced in overall slab thickness. Even though CCS system is widely used in building, no study has been performed to investigate the performance of CFRP in composite deck slab system. Therefore, the main objective of this study is to experimentally investigate the efficiency of using CFRP laminates to strengthen a continuous composite deck-slab (CCS) system in the hogging zone specifically. This research proposes the use of CFRP laminate in the deck slab to enhance both cracking and yield load carrying capacity at the negative moment region. Four specimens with two equal spans were tested in this research under static loading. The failure modes, moment-deflection behaviour, load carrying capacity, and energy absorption are presented and discussed in detail.

2. Experimental Investigation

2.1. General description

Four specimens of continuous composite concrete-deck slab consisting of two spans were tested under static load. These specimens were prepared to investigate the effects of unidirectional CFRP laminate when applied in the hogging moment region. The CFRP laminate was applied on the top of concrete at the intermediate support, as shown in Fig. 1. One specimen was tested as a control slab without the CFRP strengthening effect. Three specimens were strengthened with varied lengths of CFRP laminates, as described in Table 1. The letters "CCS" refer to the continuous composite slab, and the notation "1.0L", "1.4L", and "1.7L" represents the total length of CFRP applied to each specimen, where L is referred to span length of the composite slab. All specimens were tested with a total effective slab span of 3600 mm, support to support. Full interaction between the profile steel sheet and the concrete has been considered for all specimens and was achieved by welding four shear studs to the steel plate of the intermediate support directly underneath the profile steel sheets to represent the top flange of the steel beam usually used in the construction of composite slab [5].

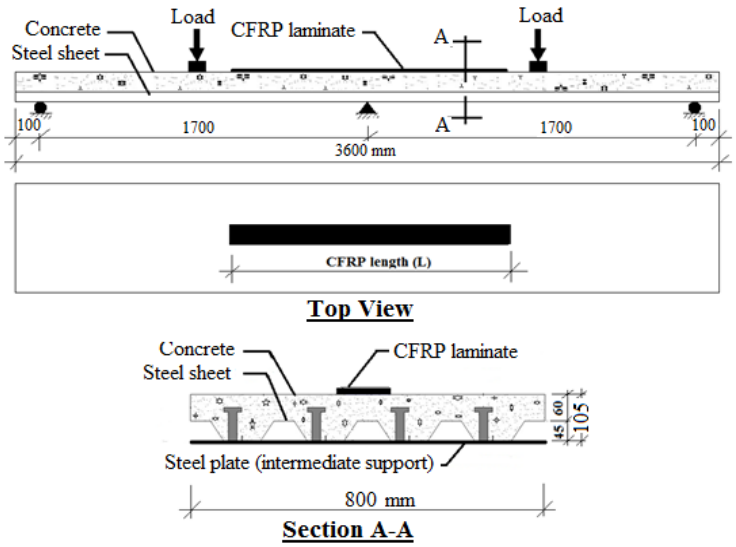

Fig. 1. The specimens of the strengthened continuous composite slab (all dimensions in millimetres).

Table 1. Specimens specifications.

Specimen ID	CFRP length (L) (mm)	Concrete compressive strength (f_{cu}) (MPa)	Slab Width (mm)	Slab Thickness (mm)	Effective slab length (mm)
CCS	–	30.2	800	105	3600
CCS-1.0L	1000	29.8	800	106	3600
CCS-1.4L	1400	29.3	800	104	3600
CCS-1.7L	1000	30 .1	800	105	3600

2.2. Material properties

In this study, profiled steel sheet type PEVA 45 [11] with a thickness of 1 mm was used, as shown in Fig. 2. The Young's modulus, tensile yield strength, and ultimate tensile strength of the profile steel sheet were equal to 210 GPa, 380 MPa, and 440 MPa, respectively, where the average was obtained from tensile testing of three coupons.

The ratio of concrete mix components designed to achieve a compressive strength of 30 MPa was 1:1.5:3 by weight. The water/cement ratio adopted for the concrete mix was 0.43. Four cubes (150 × 150 × 150 mm) were cast and cured properly in order to evaluate the compressive strength of concrete (one cube for each specimen).

The unidirectional CFRP laminate type Sika CarboDur S1012 with a width of 100 mm was used for the purpose of strengthening. Three flat coupons were cut and tested for direct tensile loading. The adhesive material Sikadur 30 was used as epoxy material to bond the CFRP laminate with the concrete part. This adhesive material is a mix of resin (A) and hardener (B) in a ratio equal to 2:1 by weight, respectively. Table 2 presents the average physical properties which were measured

in the CFRP coupons test, in addition to the nominal properties of epoxy material given by the manufacturer [12].

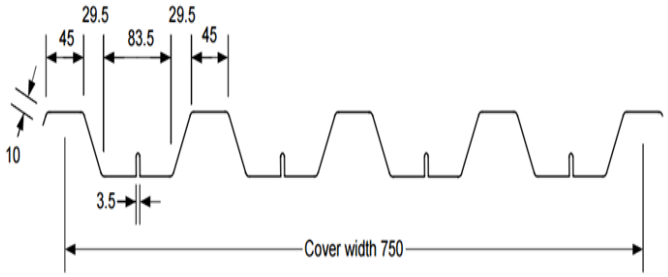

Fig. 2. Details of the profiled steel sheet (all dimensions in millimetres).

Table 2. CFRP and epoxy material properties.

Material	Thickness, t (mm)	Tensile Strength f_t (MPa)	Ultimate Strain, ε (%)	Modulus of Elasticity E (GPa)
CFRP Laminate	1.2	2800	1.7	165
Epoxy	–	24.8	1.0	4.48

2.3. Specimen preparation

Wood formwork was prepared as a permanent shutter around the profiled steel sheet during the concrete casting work. Before casting the concrete, the shutter was coated with oil on the inside (surface contact with concrete), and the profile steel sheet was cleaned before casting the concrete. Wire steel mesh was also provided to control the shrinkage of concrete. Reinforcement bars 6 mm in diameter, with a spacing of 200 mm between bars in both directions, were placed 25 mm from the top surface of the concrete. The concrete mixture was directly cast in situ and compacted with a poker vibrator. All specimens were cured for a minimum of 28 days at room temperature. The CFRP laminate was placed longitudinally parallel to the specimen's direction along the suggested lengths after 28 days of curing (1.0, 1.4, and 1.7 m); see Fig. 3.

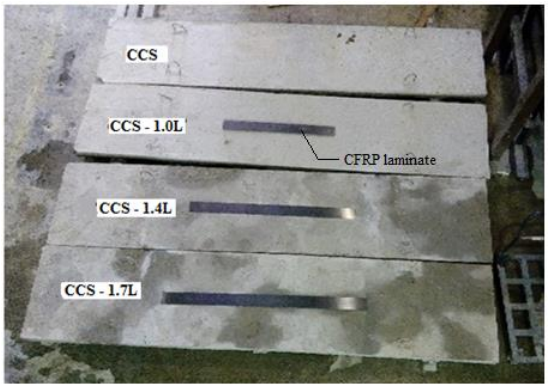

Fig. 3. The CCS specimens with the CFRP laminates.

Prior to bonding the CFRP laminate with concrete using the epoxy material, the top surface of the concrete was prepared by grinding the bonding area using in order to obtain a flat, level, and rough surface. Immediately before applying the epoxy (adhesive material), the surface of the concrete was cleaned to remove any dust and small loose particles. The adhesive material (epoxy) was mixed carefully in accordance with the manufacturer's requirements using a low-speed drill with a suitable spiral for 3 minutes until the mix became grey in colour and then directly applied on the required area (bonded surface). The prepared mixture of epoxy was spread over the bonded surface up to a thickness of approximately 1 mm. Then the CFRP laminate was immediately placed in the suggested location over the required length. A special ribbed roller was used directly after applying the CFRP laminates to remove the air voids of the epoxy and also to obtain a uniform thickness of adhesive layer as far as possible. After bonding the CFRP, the specimens were cured at room temperature for 14 days before starting the tests.

2.4. Test setup and loading procedure

The specimens were tested under five point bending loads, which were fixed to the three adjustable supports under load actuator as illustrated in Fig. 4. Rigid 'I' beam sections' were used to transfer the loads from actuator to the two steel beams tube arranged to transfer and distribute the loads to the specimens. Another two circular rigid steel beam were used as exterior roller support and one square steel tube was used as interior pinned support. The experiment was carried out in the Structural Lab of Civil Engineering Department of Universiti Kebangsaan Malaysia (UKM). The steel frame structure has a dimension of 3600 mm in length, 2600 mm in height and 1200 mm in width, fixed to the laboratory floor. Hydraulic actuator model Power Team (C10010C) with a total capacity of 1000 kN was fixed at the top-middle of the steel frame. Manual hydraulic jack was connected to the actuator in order to transfer the load gradually to the specimens through the rigid beam.

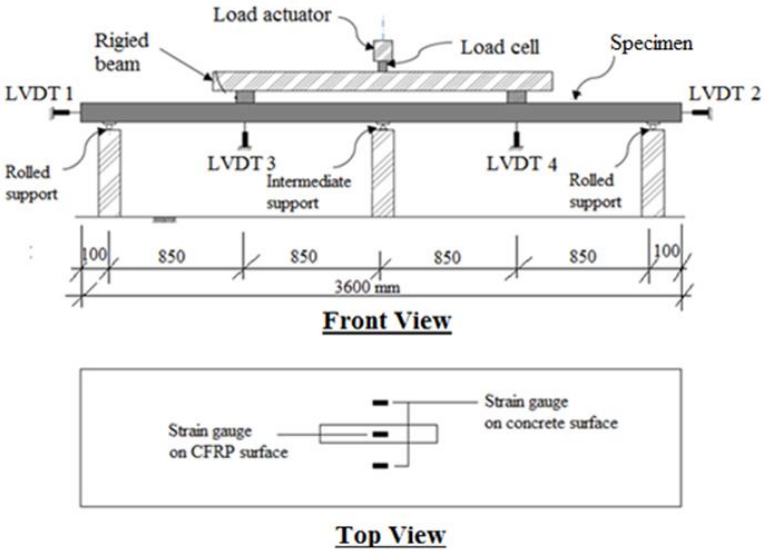

Fig. 4. Test setup and instrumentation (all dimension in mm).

3. Test Results and Discussion

3.1. Failure modes

In general, the specimens were loaded beyond the limit of their maximum capacity to further understand the behaviour of the CCS when strengthened with CFRP laminates at the extreme loading stage. In the CCS control specimen, tensile concrete cracking failure was observed and recorded in the intermediate support region, as shown in Fig. 5. The concrete cracks in the intermediate support region occurred due to the high tensile stress in the hogging moment area and because only shrinkage reinforcement was installed in this region to carry and resist the negative moment. During the increase in the applied loads (load increment), current crack growth and more new cracks appeared, the width of existing cracks become wider, indicating the extreme failure of the specimen, and then the load value starts to gradually decrease.

Generally, the concrete of the control specimen cracked at an earlier loading stage compared to the strengthened specimens due to the effects of the CFRP laminates laid in the tensile zone (the top of the concrete at the intermediate support). However, debonding failure between the CFRP laminate and concrete was exhibited by the strengthened specimens, as shown in Fig. 6 for specimen CCS-1.0L as an example).

A cracking sound was first heard in the pure-tension region, indicating that debonding failure between the CFRP laminates and concrete had started to occur, specifically when the strengthened specimens reached about 90-95% of their ultimate load capacity. After that, a rapid release of the specimen's energy occurred; at this point, the CFRP laminate totally debonded from one side and the slab cracks became much wider than before, causing a sudden drop in the load capacity. Before the full debonding failure occurred, an initial concrete crack started from the edge over the intermediate support as a straight line (perpendicular to the CFRP position), and then as the test load increased, these straight cracks become a little wider and other small inclined cracks surrounding the CFRP laminates started to occur (see Fig. 6), but due to the restraint provided by the CFRP laminate, these cracks remained limited until the final debonding failure took place.

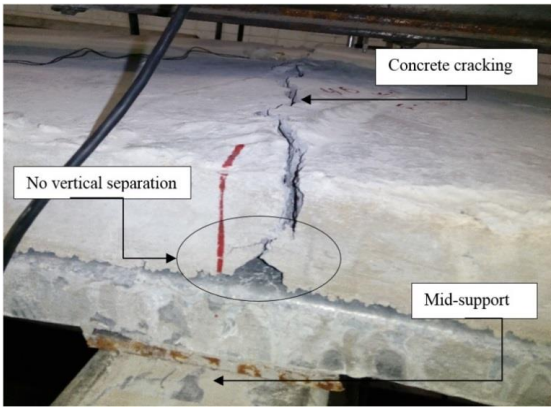

Fig. 5. Concrete cracking failure of CCS specimens in the hogging region.

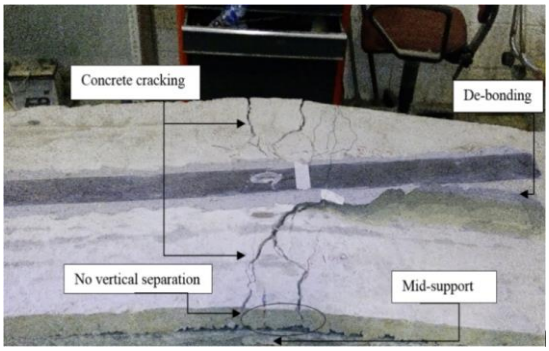

Fig. 6. Debonding failure of specimen CCS-1.0L.

Table 3 summarizes the failure modes, ultimate moment capacity (M_u), and the moment value when the CFRP debonding occurred (M_d), LIR and EA. Moreover, increasing the CFRP laminates' length delayed the debonding failure but could not prevent this type of failure from occurring, which may be attributed to the huge amount of peeling stress that occurred along the bonding surfaces between the CFRP and concrete surface due to the large bending stress in this region.

3.2. Moment behaviour

The moment versus mid-span deflection curves of the specimens is presented in Fig. 7. The curves behaved linearly up to the point (a), but once the loading reached this point, the concrete started to crack in the hogging moment region. Then, the specimens' stiffness decreased gradually with increasing loading values due to the effects of these cracks until the point (b), where the debonding failure between the CFRP and concrete started to occur in the strengthened specimens. Then, as a final stage, the load capacity of the specimens dropped rapidly, allowing the ultimate capacity to be recorded. In general, after point (a), the load value of the CCS control specimen dropped significantly due to the small number of reinforcement bars used in the tension zone, while the specimens CCS-1.0L, CCS-1.4L, and CCS-1.7L showed limited drops in their load values at point (a) since they were externally strengthened by the CFRP laminates. Furthermore, Fig. 8 shows the relationships between the hogging moment and the end slip of concrete from the profiled steel (the average readings from LVDTs 1 and 2). The curves in this figure confirmed that the strengthened slabs with CFRP laminate significantly improved the concrete end-slip behaviour.

3.3. Energy absorption

The energy absorption (EA) capacity of the tested CCS specimens including those strengthened with CFRP laminates was investigated and is discussed in this section. The EA values are usually estimated by calculating the area under the curve of load versus deflection for the tested specimens following the same concept as in [13]. Generally, based on the total area under the curve, all the strengthened CCS specimens with CFRP laminates absorbed more energy than the unstrengthened specimen (CCS control specimen), as shown in Fig. 9. The EA capacity values of the tested specimens are presented in Table 3 as well. Compared to all the strengthened

CCS specimens, the CCS control specimen has the lowest EA capacity of about 2559.3 kN.mm. This value increased to 3142.2 kN.mm (+23%) and 3410.3 kN.mm (+33%) when the same slab was strengthened in the hogging region by CFRP laminates along lengths of 1.0 and 1.4 m, respectively, for the specimens CCS-1.0L and CCS-1.4L. Since the specimen, CCS-1.7L achieved the highest load value; its EA capacity was the highest, at 3836.9 kN.mm, which is about 50% higher than the value of the control specimen. This finding confirmed that the EA capacity increased with increasing CFRP length.

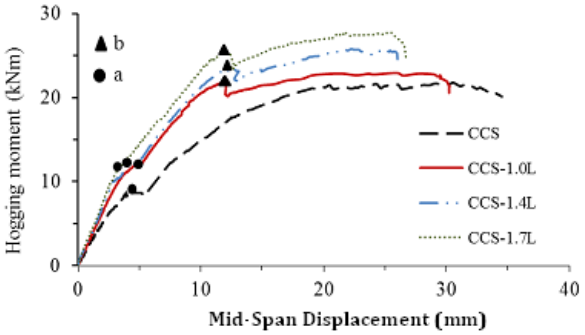

Fig. 7. Moment versus mid-span displacement relationships.

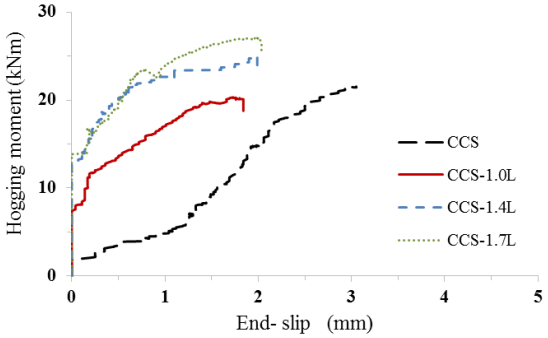

Fig. 8. Moment versus end-slip relationships.

Table 3. Experimental results of failure mode and load capacity.

Specimens ID.	Failure mode	M_u kN.m	M_d kN.m	LIR	EA (kN.mm)
CCS	Concrete cracking at the intermediate support	21.5	–	–	2559.3
CCS-1.0L	Concrete cracking at the intermediate support, then debonding failure	23.0	21.3	1.06	3142.2
CCS-1.4L	Concrete cracking at the intermediate support, then debonding failure	25.8	23.1	1.18	3410.3
CCS-1.7L	Concrete cracking at the intermediate support, then debonding failure	27.9	24.15	1.28	3836.9

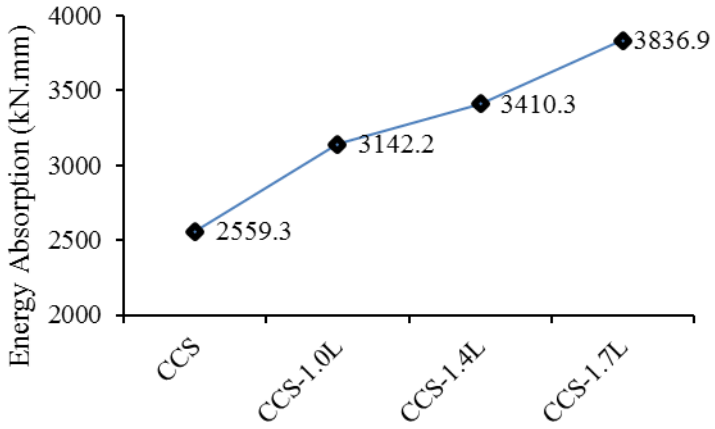

Fig. 9. Energy absorption capacity.

4. Conclusion

Experimental has been carried out in this research to investigate the performance of continuous composite slab (CCS) when strengthened in the hogging region by CFRP laminates/plates. The conclusions obtained from the test can be summarized as follows:

- In general, strengthening the CCS specimen in the hogging region (the top surface of the concrete at the internal support) with CFRP laminates significantly improved its moment capacity.
- For all the strengthened CCS specimens, debonding failure occurred between the CFRP and the concrete surfaces at a certain loading limit (higher than the load capacity of the corresponding control specimen). However, increasing the CFRP length was insufficient to preventing debonding failure from occurring, although it delayed this failure somewhat. Thus, the CCS specimens strengthened with a CFRP length of 1.7 m achieved a higher load improvement ratio than those strengthened with CFRP lengths of 1.4 and 1.0 m, respectively.
- The CFRP plates improved the capability of the CCS specimens to absorb more energy in general, and all the strengthened CCS specimens absorbed more energy than their control specimens. The energy absorption capacity of the specimen strengthened with a CFRP length of 1.7 m achieved a higher value than the specimens strengthened with CFRP lengths of 1.4 and 1.0 m, respectively.
- For further study, FEA-methods can be used to analyze the effect of CFRP thickness and numbers, slab span length and width, and concrete strength.

Acknowledgements

The authors would like to express their gratitude to Ministry of Higher Education (MOHE) and Universiti Kebangsaan Malaysia (UKM) for providing funding to this project with the grant no. FRGS/2/2013/TK02/UKM/02/1.

References

1. Chen, S. (2003). Load carrying capacity of composite slabs with various end constraints. *Journal of Constructional Steel Research*, 59(3), 385–403.
2. EC4. (2004). 1-1. *Eurocode 4: design of composite steel and concrete structures-Part 1.1: General rules and rules for buildings*. European Committee for Standardization.
3. Majdi, Y.; Hsu, C.-T.T.; and Punurai, S. (2014). Local bond-slip behaviour between cold-formed metal and concrete. *Engineering Structures*, 69(6), 271-284.
4. Poh, K.W.; and Attard, M.M.; (1993). Calculating the load-deflection behaviour of simply-supported composite slabs with interface slip. *Engineering Structures*, 15(5), 359-367.
5. Abas, F.M.; Gilbert, R.I.; Foster, S.; and Bradford, M. A. (2013). Strength and serviceability of continuous composite slabs with deep trapezoidal steel decking and steel fibre reinforced concrete. *Engineering Structures*, 49(4), 866-875.
6. Gholamhoseini, A.; Gilbert, I.; and Bradford, M. (2013). Ultimate strength of continuous composite concrete slab. *Proceedings of the 7th International Conference on Composite Construction*. North Queensland, Australia.
7. Ackermann, F.P.; and Schnell, J. (2008). Steel Fibre Reinforced Continuous Composite Slabs. *Proceedings of the International Conference on Composite Construction in Steel and Concrete*. Colorado, United States of America, 125-137.
8. Ashour, A.; El-Refaie, S.; and Garrity, S. (2004). Flexural strengthening of RC continuous beams using CFRP laminates. *Cement and Concrete Composites*, 26(7), 765-775.
9. Kim, J.J.; Noh, H.-C.; Reda Taha, M.M.; and Mosallam, A. (2013). Design limits for RC slabs strengthened with hybrid FRP–HPC retrofit system. *Composites Part B: Engineering*, 51, 19-27.
10. El-Shihy, A.M.; Fawzy, H.M.; Mustafa, S.A.A.; and Elzohairy, A. (2010). Experimental and numerical analysis of composite beams strengthened by CFRP laminates in hogging moment region. *Steel and Composite Structures*, 10(3), 281-295.
11. AJIYA Berhad, (2015). PEVA 45. Retrieved March 5, 2017, from http://www.ajiya.com/structural-products/.
12. SIKA Malaysia, (2016). Retrieved March 5, 2017, from https://mys.sika.com/en/solutions_products/download/construction-pds.html.
13. Hosseinpour, E.; Baharom, S.; Badaruzzaman, W.H.W.; Shariati, M.; and Jalali, A. (2018). Direct shear behavior of concrete filled hollow steel tube shear connector for slim-floor steel beam. *Steel and Composite Structures*, 26(4), 485-499.